Stoichiometry and Kinetics of *p*-Methoxytoluene Oxidation by Electron Transfer. Mechanistic Dichotomy between Side Chain and Nuclear Substitution

C. J. Schlesener and J. K. Kochi*

Department of Chemistry, Indiana University, Bloomington, Indiana 47405

Received December 29, 1983

The oxidation of *p*-methoxytoluene by tris(phenanthroline)iron(III) or $Fe(phen)_3^{3+}$ in acetonitrile containing pyridine bases affords both side chain and nuclear substitution products in the form of the isomeric *N*-benzylpyridinium ion I and *N*-anisylpyridinium ion II, respectively. The relative rates of formation of I and II show an unusual and pronounced dependence on the structure of the base—pyridine yielding mainly II, and 2,6-lutidine producing exclusively I. The mechanistic dichotomy between these side chain and nuclear substitution products is resolved by the complete analysis of the complex oxidation kinetics. Thus the mechanism in Scheme II involves initial electron transfer from *p*-methoxytoluene to $Fe(phen)_3^{3+}$ to afford the *p*-methoxytoluene cation radical [$PMT^{+\cdot}$] as a reactive intermediate which can be directly observed by transient ESR spectroscopy. Products I and II arise from [$PMT^{+\cdot}$] and the pyridine base in a follow-up step with a second-order rate constant k_2. The base dependence of k_2 together with the deuterium kinetic isotope effect for deprotonation help to delineate the separate transition states leading to side chain and nuclear substitution. The kinetics also allow the evaluation of the rate constant k_1 for electron transfer from *p*-methoxytoluene to $Fe(phen)_3^{3+}$. The correlation of log k_1 with analogous values for electron transfer from a series of polymethylated benzenes according to the linear free energy relationship from the Marcus rate theory shows the essential outer sphere character of the transition state for electron transfer.

Introduction

The oxidation of aromatic compounds either by transition metal complexes or electrochemical methods has attracted increasing attention as a route to the introduction of various functional groups.[1] Among these studies, the oxidative transformation of an alkyl substituent, particularly a methyl group, has been investigated at length since it bears directly on the industrially important conversion of *p*-xylene to terephthalic acid.[2] Two major pathways have been identified in the oxidation of aralkanes—namely side chain and nuclear substitution as given below with toluene as an illustrative example.[3] This dichotomy has

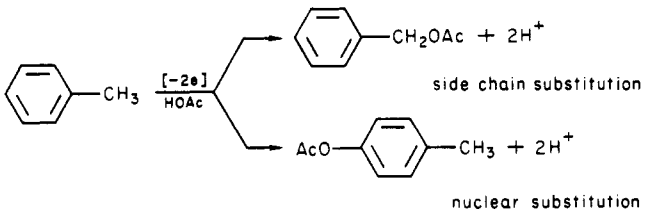

been identified in most of the previous studies of aromatic oxidations by extensive product studies using various types of alkyl aromatic hydrocarbons.[1,4]

Electron transfer as a primary act in the oxidation of aromatic compounds was first proposed by Dewar and co-workers[5] in their pioneering investigation of *p*-methoxytoluene (PMT) with manganese(III) acetate as the oxidant. Their kinetic studies which established the inverse dependence on manganese(II) led to the postulation of the cation radical of *p*-methoxytoluene as the reactive intermediate. According to the mechanism in Scheme I,

Scheme I

$$ArCH_3 + Mn^{III} \underset{}{\overset{K}{\rightleftharpoons}} ArCH_3^{+\cdot} + Mn^{II} \quad (a)$$

$$ArCH_3^{+\cdot} \xrightarrow{k} ArCH_2\cdot + H^+ \quad (b)$$

$$ArCH_2\cdot + Mn^{III} \xrightarrow{fast} ArCH_2^+ + Mn^{II} \quad (c)$$

$$ArCH_2^+ + HOAc \xrightarrow{fast} ArCH_2OAc + H^+ \quad (d)$$

side chain substitution proceeds by an initial reversible electron transfer (step a), followed by a slow rate-limiting proton transfer (step b). Indeed, a complete kinetic analysis of this mechanism has been recently carried out by Eberson for PMT by using the heteropoly cobaltotungstate $K_5CoW_{12}O_{40}$ as the oxidant.[6]

Our interest in PMT arises from the desire to exploit tris(phenanthroline)iron(III) or $Fe(phen)_3^{3+}$ as an oxidant,[7] since it has a number of desirable properties for mechanistic studies of organic oxidation. Thus it is a reasonably potent oxidant (E°_{Fe} = 1.09 V vs. SCE in CH_3CN), but more importantly it is substitution inert and prone to undergo electron transfer by an outer sphere mechanism.[8] In this study we wish to describe how $Fe(phen)_3^{3+}$ can be utilized in the oxidation of this prototypical methylarene[9]

* Present address: Department of Chemistry, University of Houston, University Park, Houston, Texas 77004.

(1) (a) Beletskaya, I. P.; Makhon'kov, D. I. *Russ. Chem. Rev.* **1981**, *50*, 534. (b) Tomilov, A. P. *Ibid.* **1961**, *30*, 639.

(2) For a review, see: Sheldon, R. A.; Kochi, J. K. "Metal-Catalyzed Oxidation of Organic Compounds"; Academic Press: New York, 1982; Chapters 5 and 10.

(3) (a) Eberson, L.; Nyberg, K. *J. Am. Chem. Soc.* **1966**, *88*, 1686. (b) Eberson, L.; Nyberg, K. *Acc. Chem. Res.* **1973**, *6*, 106. (c) For the toluene cation radical, see: Komatsu, T.; Lund, A.; Kinell, P.-O. *J. Phys. Chem.* **1972**, *76*, 1721.

(4) (a) Heiba, E. I.; Dessau, R. M. Koehl, W. J., Jr. *J. Am. Chem. Soc.* **1969**, *41*, 6830. (b) Hanotier, J.; Hanotier-Bridoux, M.; de Radzitzky, P. *J. Chem. Soc., Perkin Trans. 2* **1973** 381. (c) Ross, S. D.; Finkelstein, M.; Petersen, R. C. *J. Org. Chem.* **1970**, *35*, 781. (d) Blum, Z.; Cedheim, L.; Nyberg, K. *Acta Chem. Scand., Ser. B* **1975**, *B29*, 715. (e) Shaw, M. J.; Weil, J. A.; Hyman, H. H.; Filler, R. *J. Am. Chem. Soc.* **1970**, *92*, 5096. (f) Shaw, M. J.; Hyman, H. H.; Filler, R. *J. Org. Chem.* **1971**, *36*, 2918. (g) Eberson, L.; Oberrauch, E. *Acta Chem. Scand., Ser. B* **1981**, *B35*, 193.

(5) Andrulis, P. J.; Dewar, M. J. S.; Dietz, R.; Hunt, R. L. *J. Am. Chem. Soc.* **1966**, *88*, 5473.

(6) Eberson, L. *J. Am. Chem. Soc.* **1983**, *105*, 3192.

(7) Schilt, A. A. "Analytical Applications of 1,10-Phenanthroline and Related Compounds"; Pergamon: Oxford, 1969.

(8) See, e.g.: (a) Dulz, G.; Sutin, N. *Inorg. Chem.* **1963**, *2*, 917. (b) Diebler, H.; Sutin, N. *J. Phys. Chem.* **1964**, *68*, 174. (c) Wilkins, R. G.; Yelin, R. E. *Inorg. Chem.* **1968**, *7*, 2667. (d) Wong, C. L.; Kochi, J. K. *J. Am. Chem. Soc.* **1979**, *101*, 5593. (e) Fukuzumi, S.; Wong, C. L.; Kochi, J. K. *J. Am. Chem. Soc.* **1980**, *102*, 2928.

(9) For some examples of oxidation studies of PMT and related compounds using chemical oxidants and electrochemical methods, see: (a) Eberson, L. *J. Am. Chem. Soc.* **1967**, *89*, 4669. (b) Eberson, L.; Jönsson, L.; Wistrand, L.-G. *Acta Chem. Scand., Ser. B* **1978**, *B32*, 520. (c) Nyberg, K.; Wistrand, L.-G. *J. Org. Chem.* **1978**, *43*, 2613. (d) Marrocco, M.; Brilmyer, G. *J. Org. Chem.* **1983**, *48*, 1487. (e) Nilsson, A.; Palmguist, U.; Petterson, T.; Ronlan, A. *J. Chem. Soc., Perkin Trans. 1* **1978**, 708. (f) Uemura, S.; Ikeda, T.; Tanaka, S.; Okano, M. *J. Chem. Soc., Perkin Trans. 1* **1979**, 2574.

0022-3263/84/1949-3142$01.50/0

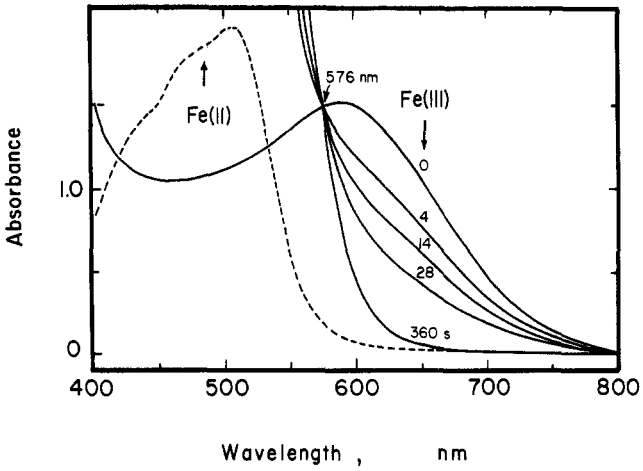

Figure 1. Spectral changes during the oxidation of 1.9×10^{-2} M of *p*-methoxytoluene by 2.0×10^{-3} M $Fe(phen)_3^{3+}$ in acetonitrile containing 3.1×10^{-2} M pyridine and 0.1 M $LiClO_4$. Initial iron(III) indicated as O. Numbers refer to time, t = 4, 14, 28, and 360 s after mixing. The final spectrum of iron(II) indicated by dashed line, was recorded after the reaction mixture was diluted ~12-fold.

to afford second-order rate constants for the formation of the cation radical, as well as the second-order rate constants for its deprotonation by pyridine bases. Moreover the latter allows the mechanism of the side chain and the nuclear substitution of PMT to be delineated in a quantitative manner.

Results

The oxidation of *p*-methoxytoluene (PMT) by tris(phenanthroline)iron(III) in acetonitrile solution containing pyridine as an added base is accompanied by the rapid change in color from blue to red. The distinctive color change is indicative of the reduction of the iron(III) complex $Fe(phen)_3^{3+}$ to the iron(II) complex $Fe(phen)_3^{2+}$.[7] The course of oxidation is illustrated by the temporal changes in the absorption spectrum during PMT oxidation in Figure 1. Note the absorption spectrum (dashed curve) at the end of the oxidation corresponds to that of the reduced ferrous complex $Fe(phen)_3^{2+}$.

Stoichiometry and Products of PMT Oxidation by Iron(III). The stoichiometry for the iron(III) oxidation of *p*-methoxytoluene was determined by two independent methods involving (a) the reduction of the iron(III) complex and (b) the disappearance of the methylarene. The reduction of the iron(III) complex was determined quantitatively by spectral titration using the method of continuous variations[10] of $Fe(phen)_3^{3+}$, as monitored at 560 nm (see the Experimental Section). The consumption of PMT was measured directly by quantitative gas chromatography using the internal standard method. The results from the spectral titration and the gas chromatographic analysis indicated a ratio of 2.1 and 1.8, respectively, for the relative amount of iron(II) and PMT consumed. Accordingly, the stoichiometry corresponds to an overall 2-electron oxidation, viz.,

$$p\text{-}CH_3C_6H_4OCH_3 + 2Fe(phen)_3^{3+} \xrightarrow{[B]} [p\text{-}CH_3C_6H_4OCH_3]_{ox} + 2Fe(phen)_3^{2+} \quad (1)$$

where the quantity in brackets represents the oxidation products of *p*-methoxytoluene to be described below.

(10) Rossotti, F. J. C.; Rossotti, H. "Determination of Stability Constants"; McGraw-Hill, Inc.: New York, 1961; p 47.

Table I. Oxidation Products of *p*-Methoxytoluene by Tris(phenanthroline)iron(III) in the Presence of Pyridine and 2,6-Lutidine as Added Bases[a]

base [B] (mmol)	*p*-methoxytoluene initial (mmol)	*p*-methoxytoluene final (mmol)	$Fe(phen)_3^{3+}$ initial (mmol)	$Fe(phen)_3^{3+}$ final (mmol)	products,[b] mol (%)
pyridine (1.01)	0.50	0.11	1.00	0.05	Ia 0.04_5 (9) IIa 0.35 (69)
2,6-lutidine (1.00)	0.50	0.25	1.00	0.33	IIb 0 (<3) Ib 0.19 (38)

[a] In 20 mL of acetonitrile at 25 °C with $Fe(phen)_3(PF_6)_3$. [b] Yield based on initial PMT. Estimated error of ±10% in the NMR analysis.

In order to identify the organic products of oxidation, the reaction was carried out on a larger scale and allowed to stand for a prolonged period prior to analysis. Small aliquots of the reaction mixtures were initially examined by ^1H NMR spectroscopy, and they revealed spectral changes which were characteristic of the base employed. Thus the oxidation in the presence of 2,6-lutidine resulted in the appearance of a pair of new singlet resonances at δ 5.7 and 3.7 along with the diminution of the methoxy and methyl resonances of PMT at δ 3.6 and 2.2, respectively. By contrast, the same oxidation in the presence of pyridine led to the appearance of a pair of new resonances at δ 3.8 and 2.4 indicative of another methoxytoluene derivative. Subsequent workup of the reaction mixture and isolation of the products afforded two types of products, I and II, corresponding to oxidative, side chain substitution and nuclear substitution, respectively, of PMT.

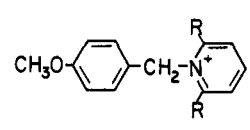

Ia, R = H
Ib, R = CH_3

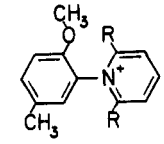

IIa, R = H
IIb, R = CH_3

The *N*-benzylpyridinium salts Ia and Ib were independently synthesized by the Menschutkin reaction of *p*-methoxybenzyl bromide with pyridine and 2,6-lutidine, respectively. An authentic sample of the *N*-arylpyridinium salt IIa was synthesized by cleavage of *N*-(2,4-dinitrophenyl)pyridinium chloride with 5-methyl-2-anisidine, followed by ring closure and elimination according to Marvell's procedure.[11] The identity of the reaction products with the authentic samples of the *N*-benzylammonium Ia and Ib and the *N*-arylpyridinium salt IIa was confirmed by comparison of their ^1H and ^{13}C NMR spectra.

Analysis of the reaction mixtures by quantitative ^1H NMR spectroscopy using 1,3,5-tri-*tert*-butylbenzene as an internal reference (see Experimental Section) indicated that the nuclear-substituted *N*-anisylpyridinium salt IIa was the predominant product when pyridine was the base, whereas the side chain substituted *N*-benzylpyridinium salt Ib was the exclusive product when 2,6-lutidine was the base. Although an authentic sample of the *N*-anisyllutidinium salt IIb was not independently synthesized, we could readily infer that it was not a significant oxidation product judging from the absence of a downfield shifted methyl resonance expected at δ 2.4 by analogy with that of the analogous arylpyridinium salt IIa. The yields of each product are included in Table I for some typical oxidations

(11) Marvell, E. N.; Shahidi, I. *J. Am. Chem. Soc.* **1970**, *92*, 5646.

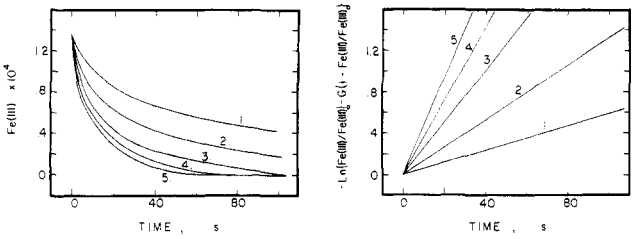

Figure 2. (a) The rate of disappearance of 1.33×10^{-4} M Fe(phen)$_3^{3+}$ in the presence of 1.85×10^{-2} M *p*-methoxytoluene in acetonitrile containing 0.1 M $LiClO_4$ and various amounts of added pyridine (1) 1.24×10^{-2} M, (2) 3.10×10^{-2} M, (3) 6.2×10^{-2} M, (4) 9.27×10^{-2} M, (5) 1.24×10^{-1} M. (b) The rate data in (a) plotted as the function in eq 2.

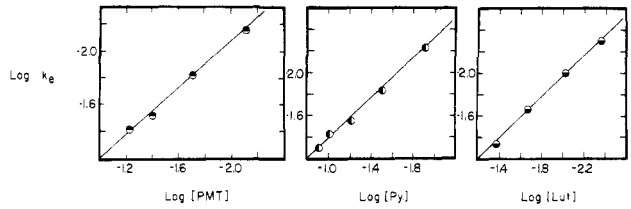

Figure 3. The dependence of the experimental rate constant k_e for oxidations with 1.3×10^{-4} M Fe(phen)$_3^{3+}$ on the concentration of (a) *p*-methoxytoluene [3×10^{-2} M py], (b) pyridine [1.9×10^{-2} M PMT], and (c) 2,6-lutidine [1.9×10^{-2} M PMT].

of PMT. [Note the excessive consumption of the iron(III) complex arose from the background reaction with the solvent and/or the added base upon prolonged standing.]

Rates of PMT Oxidation by Iron(III). The oxidation of *p*-methoxytoluene by Fe(phen)$_3^{3+}$ in acetonitrile is characterized by a rather fast initial decrease in the iron(III) titer, followed by a leveling off to a plateau corresponding to less than 20% of that required for the stoichiometry in eq 1. However, the presence of either pyridine or 2,6-lutidine (added in amounts which were at least equivalent to PMT) promoted the completion of PMT oxidation in the rather pronounced manner shown in Figure 2a. Accordingly, all of the rate studies were carried out with these bases added in excess to approximate zero-order kinetic conditions.

The rates of oxidation were measured by following the decrease in the iron(III) concentration spectrally at 650 nm (ϵ 540 M^{-1} cm^{-1}) in acetonitrile solution containing 0.1 M lithium perchlorate to maintain constant ionic strength. The disappearance of iron(III) in the presence of PMT in molar excess followed the rate expression in eq 2 (to be

$$-\ln\frac{[\mathrm{Fe(III)}]}{\mathrm{Fe(III)}]_0} - 1 + \frac{[\mathrm{Fe(III)}]}{[\mathrm{Fe(III)}]_0} = k_e t \qquad (2)$$

derived later), as shown in Figure 2b by the linear plots with slopes k_e obtained at various initial concentrations of the pyridine base. The change in the experimental rate constant k_e with variations in the initial concentration of *p*-methoxytoluene, pyridine, and 2,6-lutidine [all in molar excess relative to iron(III)] is plotted in Figure 3 parts a, b, and c, respectively. The slopes of unity in each of these graphs establish the first order dependence of the experimental (i.e., pseudo-first-order) rate constant k_e on the concentrations of PMT and pyridine or 2,6-lutidine.

Deuterium Isotope Effect on the Rates of PMT Oxidation. The rates of iron(III) oxidation were determined under the same conditions by using *p*-methoxytoluene specifically labelled with a deuteriated methyl group on the ring, i.e., $CH_3OC_6H_4CD_3$. The second-order rate constants are given in Table II for the oxidation of *p*-$CH_3OC_6H_4CH_3$ and *p*-$CH_3OC_6H_4CD_3$ which were carried out with either pyridine or 2,6-lutidine as the added base.

Table II. Comparative Rates of Oxidation of *p*-Methoxytoluene and Its α,α,α-Trideuterio Derivative with Fe(phen)$_3^{3+}$ [a]

base [B]	k_H, M^{-1} s^{-1}	k_D, M^{-1} s^{-1}
pyridine	$1.7 \pm 0.2 \times 10^{-3}$	$6.2 \pm 0.2 \times 10^{-4}$
2,6-lutidine	$3.7 \pm 0.2 \times 10^{-3}$	$6.7 \pm 0.2 \times 10^{-4}$

[a] In acetonitrile solutions containing $\sim 10^{-2}$ M base, 10^{-2} M *p*-methoxytoluene, 10^{-4} M Fe(phen)$_3$(PF$_6$)$_3$, and 0.1 M $LiClO_4$ at 22 °C. Error in the rate constant indicates one standard deviation. The rate constants k_H and k_D refer to $k_e[\mathrm{Fe(III)}]_0/[\mathrm{PMT}]_0[\mathrm{B}]_0$ for *p*-$CH_3C_6H_4OCH_3$ and *p*-$CD_3C_6H_4OCH_3$, respectively, as described in eq 6 and 7.

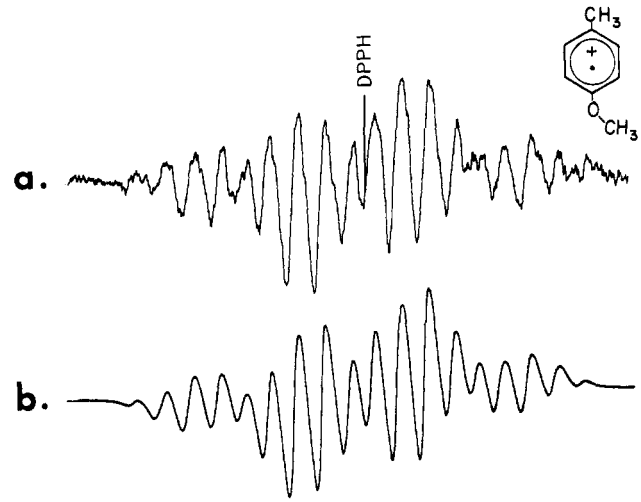

Figure 4. Upper: the X-band ESR spectrum of [PMT$^{+\cdot}$] obtained from the thermal reaction of *p*-methoxytoluene and Fe(phen)$_3^{3+}$. Lower: computer simulated spectrum of [PMT$^{+\cdot}$].[12]

The results indicate a substantial difference in the rates of PMT oxidation depending on whether pyridine or 2,6-lutidine were employed as the added base.

Discussion

The base-promoted oxidation of *p*-methoxytoluene by iron(III) under the conditions described in this study is unusual for two principal reasons. First, the results in Table I indicate that the products of oxidation which derive from either side chain and nuclear substitution (as exemplified by structures I and II, respectively) are highly dependent on whether pyridine or 2,6-lutidine is employed. Second, the results in Table II indicate that the kinetic isotope effect measured with *p*-methoxytoluene-α,α,α-d_3 is either relatively large or small depending on whether 2,6-lutidine or pyridine is the base. Since both problems relate to the nature of the base B, its role in the oxidative rate process must be defined quantitatively. We proceed by noting that the observed products, stoichiometry, kinetics, and kinetic isotope effects are akin to those derived from earlier studies of *p*-methoxytoluene oxidation,[5,6,9] in which the cation–radical [PMT$^{+\cdot}$] is the reactive intermediate formed by one-electron transfer. The validity of this premise is demonstrated by the observation of the well-resolved ESR spectrum of [PMT$^{+\cdot}$] shown in Figure 4 simply upon the exposure of *p*-methoxytoluene to Fe(phen)$_3^{3+}$.[12] The basic outline of such an electron transfer

(12) (a) Since arene cation radicals are more persistent in trifluoroacetic acid, the ESR spectra were recorded at 25 °C by mixing 1.3×10^{-3} M PMT and 2.3×10^{-3} M Fe(phen)$_3^{3+}$ in this solvent. (b) The computer simulation in Figure 4 was carried out with proton hyperfine splittings of 15.2 (4 H), 4.3 (4 H), and 3.5 (3 H) gauss, which accord with those for [PMT$^{+\cdot}$] generated by a completely independent procedure (see: Dixon, W. T.; Murphy, D. *J. Chem. Soc., Perkin Trans. 2* **1976**, 1823) $\langle g \rangle$ = 2.0033.

Scheme II

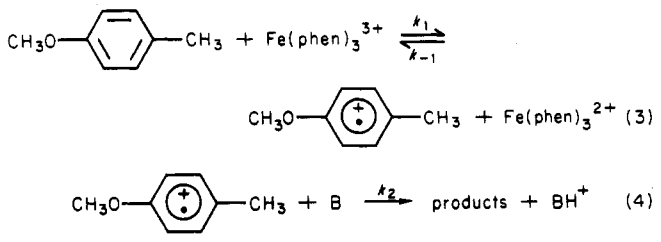

mechanism as applied to the iron(III) oxidations pertinent to this study is presented below, and each step is labeled with its appropriate rate constant. The role of the base B in Scheme II is to displace the redox equilibrium in eq 3 by proton removal in the followup reaction in eq 4. The use of the equilibrium-state approximation for [PMT^{+}·] as the transient intermediate in Scheme II leads to the following rate law.

$$-\ln\frac{[\text{Fe(III)}]}{[\text{Fe(III)}]_0} - 1 + \frac{[\text{Fe(III)}]}{[\text{Fe(III)}]_0} = 2\frac{k_1k_2[\text{PMT}]_0[\text{py}]_0}{k_{-1}\,[\text{Fe(III)}]_0}t \tag{5}$$

The brackets represent concentrations at time t, and the subscript 0 refers to the initial condition at $t = 0$. [For the derivation of eq 5 from the mechanism in Scheme II, compare with eq 29 in the Experimental Section.] Comparison of the rate law in eq 5 with the experimental kinetics in eq 2 leads to the relationship among the various rate constants as:

$$k_e = \frac{2k_1k_2}{k_{-1}}\frac{[\text{PMT}]_0[\text{py}]_0}{[\text{Fe(III)}]_0} \tag{6}$$

Thus the experimental determination of the rate constant k_e according to Figure 2 directly affords values of the intrinsic rate constant ratio k_1k_2/k_{-1}, since the quantities in brackets are constant under conditions of our kinetics experiments. This rate constant ratio is designated as k_H, i.e.,

$$k_H = k_1k_2/k_{-1} = Kk_2 \tag{7}$$

and the values listed in the second column of Table II for PMT oxidations with the pyridine and 2,6-lutidine bases. The constant K in eq 7 represents the electron-transfer preequilibrium step in eq 3, and it is independently evaluated by the standard free energy change, i.e.,

$$K = k_1/k_{-1} = \exp(\mathcal{F}[E^\circ_{Fe} - E^\circ_{Ar}]/RT) \tag{8}$$

where E°_{Fe} and E°_{Ar} represent the standard reduction potentials for the Fe(phen)$_3^{3+}$/Fe(phen)$_3^{2+}$ and the [PMT^{+}·]/[PMT] redox couples, respectively. The other terms have their usual significance. The values of E°_{Fe} and E°_{Ar} measured in trifluoroacetic acid solutions at a constant salt concentration of 0.1 M tetra-*n*-butylammonium perchlorate are 0.87 and 1.26 V vs. Ag/AgClO$_4$ at 25 °C.[13] The combination of eq 7 and 8, together with the assumption that the difference ($E^\circ_{Fe} - E^\circ_{Ar}$) is solvent independent, afford the deprotonation rate constant k_2 = 1.4×10^4 M^{-1} s^{-1}, when 2,6-lutidine is the base.

Since the value for E°_{Ar} in acetonitrile is uncertain,[13] let us consider the significance of the rate constant k_H without any assumptions. Thus it follows from eq 7 that the *relative* values of k_H for 2,6-lutidine and pyridine in Table II actually represent the ratio of deprotonation rate constants since the redox preequilibrium constant K is common with both bases, i.e.,

$$k_H{}^L k_H{}^P = k_2{}^L/k_2{}^P \tag{9}$$

where the superscipts L and P refer to 2,6-lutidine and pyridine, respectively. The relative rates of deprotonation are listed in Table III. In other words, 2,6-lutidine is more than twice as effective as pyridine in the follow-up step in eq 4. Likewise, the kinetic isotope effect reported as k_H/k_D in column 4 of Table III represents only that for the deprotonation step in eq 4, i.e.,

$$k_H/k_D = k_2(H)/k_2(D) \tag{10}$$

The conclusion expressed in eq 10 leads us now to inquire as to why the observed kinetic isotope effect of the followup reaction in eq 4 with 2,6-lutidine is almost *twice* as large as that with pyridine: The difference in basicity of 2,6-lutidine and pyridine can be ruled out as a cause of this discrepancy for the following reason. There is a recent kinetic study[14] of the hexamethylbenzene cation radical [HMB^{+}·], which is similar to [PMT^{+}·] but for which there is no ambiguity as to the role of the pyridine, namely, it functions exclusively as a base for benzylic proton removal, i.e.,

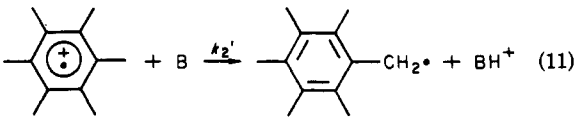

It is noteworthy that proton transfer from [HMB^{+}·] in eq 11 shows *no* difference in kinetic isotope effects between pyridine and 2,6-lutidine. The rate constants relevant to eq 4 and 10 are retabulated in Table III to facilitate a direct comparison of the behavior of [HMB^{+}·] and [PMT^{+}·] toward pyridine and lutidine bases. Indeed the results in column 3 indicate that the relative rates of reaction of both cation radicals with pyridine and 2,6-lutidine are the *same*.[15] We are thus forced to the conclusion that the rate measurements and the kinetic isotope effects for [PMT^{+}·] do not refer completely to the same activation processes. In other words, the values of the kinetic isotope effects may not pertain only to reactions involving rate-limiting proton transfer. We believe the key to the explanation of the difference in kinetic isotope effects for [PMT^{+}·] with pyridine and 2,6-lutidine to lie in the observation of two types of products I and II arising from side chain and nuclear substitution, respectively. If we assume a kinetic isotope effect of ~6 for the deprotonation

Table III. Comparative Kinetics Data for the Reactions of Hexamethylbenzene and *p*-Methoxytoluene Cation Radicals toward Pyridine and 2,6-Lutidine

methylarene cation radical	base	$k_2{}^L/k_2{}^P$	$k_2(H)/k_2(D)$[a]
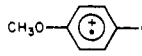	py	2.2	2.7 ± 0.3
	lut		5.6 ± 0.3
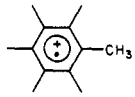	py	2.2	3.6 ± 0.3
	lut		3.9 ± 0.3

[a] The first two entries were obtained from the data in Table II by dividing the numbers in the second by the third column. The last two entries are taken from ref 24.

(13) Since the cyclic voltammogram of PMT is irreversible in acetonitrile, the oxidation potentials were measured in trifluoroacetic acid as described in the Experimental Section.

(14) Schlesener, C. J.; Amatore, C.; Kochi, J. K. *J. Am. Chem. Soc.* 1984, *106*, 3567. This paper presents a more complete kinetics analysis of arene oxidation with Fe(phen)$^{3+}$ originally examined by Fukuzumi, S.; Kochi, J. K. *J. Am. Chem. Soc.* 1982, *104*, 7599.

(15) This result is tantamount to a Hammett correlation of [HMB^{+}·] and [PMT^{+}·] with the pyridine bases in which the ρ values are the same.

rate constant k_2' of [PMT$^+$·] by pyridine,[16] i.e.,

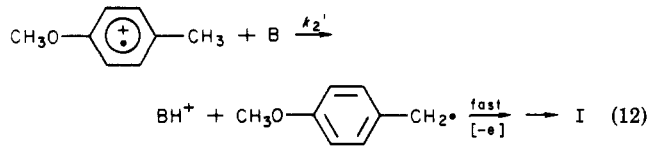

(12)

the observed value of 2.7 would imply that ~30% of the products result from benzylic proton removal, according to eq 12 (compare with eq 11), and the remainder from a process showing no kinetic isotope effect.[17] Indeed our observation of only a 12% yield of the side chain substitution product Ia accords with this formulation within the error limits of analysis. The remainder leading to nuclear substitution (see the formation of IIa in 70% yield in Table I) must then occur by a process in which proton transfer is fast. A mechanism involving the rate-limiting, nucleophilic addition of pyridine to [PMT$^+$·] with a second-order rate constant k_2'' is consistent with this formulation, i.e.,

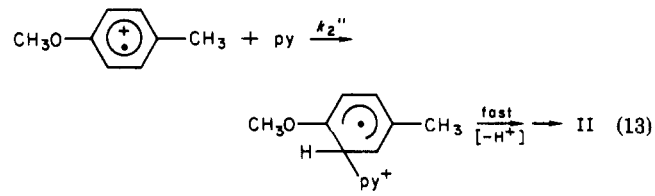

(13)

Under these circumstances the observed rate constant k_2 is actually a composite [i.e., $k_2' + k_2''$], and pyridine serves a dual capacity as a base and a nucleophile in the follow-up step in eq 4. By contrast, 2,6-lutidine primarily functions only as a Brønsted base for deprotonation of the carbon acid, since no products of nuclear substitution could be observed. In this instance, the observed kinetic isotope effect truly reflects the deprotonation process in eq 12.

Basicity vs. Nucleophilicity of Various Pyridines toward Arene Cation-Radicals. The formation of the *N*-arylpyridinium ion IIa resulting from nuclear substitution of [PMT$^+$·] was unexpected since there are only a limited number of reports of such products in the extant literature. For example, the pyridination of anthracenes and 1,4-dimethoxybenzene, which have no methyl substituents, has been observed upon anodic oxidation.[18-20] On the other hand, the cation radical of 9,10-dimethylanthracene was prone to deprotonation (i.e., benzylic substitution) rather than nucleophilic addition to the aromatic ring when a series of isomeric lutidines were employed as bases.[18] 9-Phenylanthracene shows a preference toward deprotonation rather than nucleophilic attack at a cationic tertiary carbon center (addition of a second equivalent of nucleophile), depending on the steric requirements of the base.[19] Such results identify the dichotomy which exists between nucleophilicity and basicity, as discussed by Eberson and Parker,[18,19] insofar as the reactions of aromatic cation radicals are concerned. Perhaps a better comparison might be made for this competition by considering oxidative acetoxylation and oxidative cyanation with acetate and cyanide as the base (nucleophile). Thus the oxidative acetoxylation of *p*-methoxytoluene by either chemical or anodic oxidation results almost exclusively in benzylic products derived from side chain deprotonation.[5,6,9] On the other hand, anodic cyanation of PMT in acetonitrile results in nuclear substitution to afford predominant amounts of 6-methoxy-3-tolunitrile.[21] The favored ortho addition, which is analogous to the formation of IIa from pyridine (vide supra) is consistent with the calculated charge distribution in [PMT$^+$·].[22]

The rate constants that we have been able to extract from the kinetic data coupled with the product distribution allow us to evaluate the factors involved in the competition more quantitatively. Thus the overall rate constant k_H for [PMT$^+$·] and pyridine in Table II can be corrected for the competing nuclear substitution to afford the rate constant $k_H' = 5.01 \times 10^{-4}$ M^{-1} s^{-1} for deprotonation in eq 12.[23] This value compares with that for [PMT$^+$·] and 2,6-lutidine of $k_H = 3.74 \times 10^{-3}$ M^{-1} s^{-1}, which also represents the deprotonation rate constant k_H', since nuclear substitution is nil with this base. These rate constants for the deprotonation of [PMT$^+$·] in eq 12 are related to those previously determined for [HMB$^+$·] in eq 11.[24] Indeed the two sets of rate data can be compared quantitatively with the aid of the usual Brønsted relationship,[25] i.e.,

$$k_2^{L'}/k_2^{P'} = (K_a^L/K_a^P)^\alpha \quad (14)$$

where the superscripts L and P again refer to 2,6-lutidine and pyridine, respectively. Values of K_a^L and K_a^P, the acid dissociation constants of these pyridine bases, have been independently determined in acetonitrile.[26] It is important to note that the Brønsted slope evaluated from eq 14 is $\alpha = 0.28$ for [PMT$^+$·], which is the same as that ($\alpha = 0.26 \pm 0.02$) previously determined for HMB$^+$·.[24] We therefore conclude that 2,6-lutidine and pyridine are differentiated in the deprotonation of either [PMT$^+$·] or [HMB$^+$·] only by *electronic factors* relating strictly to differences in their base strengths. By comparison, the rate constant for nucleophilic substitution of [PMT$^+$·] by pyridine in eq 13 is $k_H'' = 1.17 \times 10^{-3}$ M^{-1} s^{-1}, whereas that for 2,6-lutidine is too small to measure despite its *higher* base strength. We attribute the relatively poor nucleophilic properties of 2,6-lutidine to *steric effects* arising from a pair of *o*-methyl substituents which hinder the formation of the σ-adduct in eq 13. Such a formulation suggests a rather late transition state for nucleophilic substitution in which making the new C-N bond is important. By contrast, an early transition state pertains to the deprotonation of methylarene cation radicals by pyridine bases, since studies with [HMB$^+$·] have established the driving force to lie in the exergonic region.[24,28] Accordingly, it is noteworthy that the deprotonation rate constants are insensitive to steric effects of the pyridine bases, as expected for a process in which the making of the new bond between the proton and pyridine is minor.

Rates of Electron Transfer from PMT. The iron(III) oxidation of *p*-methoxytoluene in this study was carried

(16) This value of $k_2(H)/k_2(D)$ is close to a maximum (see the compilation in Table VIII of ref 6) related to that obtained for 2,6-lutidine (vide infra).

(17) For an analysis of the variation of the kinetic isotope effects during PMT oxidation by Ce(IV), see: Baciocchi, E.; Rol, C.; Mandolini, L. *J. Am. Chem. Soc.* **1980**, *102*, 7597.

(18) Parker, V. D.; Eberson, L. *Tetrahedron Lett.* **1969**, 2843.

(19) Parker, V. D.; Eberson, L. *Tetrahedron Lett.* **1969**, 2839.

(20) (a) Manning, G.; Parker, V. D.; Adams, R. N. *J. Am. Chem. Soc.* **1969**, *91*, 4584. (b) Lund, H. *Acta Chem. Scand.* **1957**, *11*, 1323.

(21) Yoshida, K.; Shigi, M.; Fueno, T. *J. Org. Chem.* **1975**, *40*, 63. See also: Andreades, S.; Zahnow, E. W. *J. Am. Chem. Soc.* **1969**, *91*, 4181.

(22) See also the pattern for nuclear substitution of acetate in [PMT$^+$·] during Mn(III) oxidation.[5]

(23) Note $k_H' = k_2'k_1/k_{-1}$ and $k_H'' = k_2''k_1/k_{-1}$. The value of k_H' for pyridine is obtained from the relationship: $k_H = k_H' + k_H''$ and from the product distribution in Table I that $k_2' = (30/70)k_2''$.

(24) Schlesener, C. J.; Amatore, C.; Kochi, J. K. *J. Am. Chem. Soc.*, in press.

(25) Bell, R. P. "The Proton in Chemistry", 2nd ed.; Cornell University Press, 1973; Chapter 10.

(26) Cauquis, G.; Deronzier, A.; Serve, D.; Vieil, E. *J. Electroanal. Chem. Interfacial Electrochem.* **1975**, *60*, 205.

(27) As indicated by the absence of oxidation product IIb.

(28) For the relationship between the Brønsted slope and $\alpha = 0.26$ in these experiments, see the discussion in ref 25, p 215 ff.

Table IV. Kinetic Parameters for Electron Transfer from Various Arenes to $Fe(phen)_3^{3+}$ and the Standard Oxidation Potentials of Arenes.[a]

arene	E°_{Ar}, V vs. Ag/$AgClO_4$	$\Delta G^\ddagger$, kcal mol^{-1} [b]	$\Delta G_0'$, kcal mol^{-1} [c]	$\Delta G_0^\ddagger$, kcal mol^{-1} [d]
p-$CH_3OC_6H_4CH_3$	1.26	13.9[e]	10.6	7.69
$C_6(CH_3)_6$	1.20	13.4	9.30	7.75
$C_6(CH_3)_5H$	1.33	15.6	12.3	7.61
1,2,4,5-$(CH_3)_4C_6H_2$	1.41	16.8	14.2	6.44
1,2,3,4-$(CH_3)_4C_6H_2$	1.40	18.0	13.9	9.13

[a] Rates in acetonitrile containing 0.1 M $LiClO_4$ and base (pyridine values unless stated otherwise). Oxidation potentials in trifluoroacetic acid. $E^\circ_{Fe} = 0.87$ V vs. Ag/$AgClO_4$. [b] From eq 16. [c] $\mathcal{F}(E^\circ_{Ar} - 0.87) + 1.7$ kcal mol^{-1}. [d] From eq 17. [e] Evaluated for B = 2,6-lutidine.

out by and large under conditions where the electron transfer in Scheme II (eq 3) was relatively rapid and the followup reaction(s) was rate limiting, i.e., $k_2[B] << k_{-1}[Fe(II)]$. This kinetic situation thus allowed us to concentrate our attention primarily on the product-forming steps in eq 4. Let us now consider how the well-behaved kinetics in eq 2 can be altered by higher concentrations of [B] so that the system will be forced into the kinetics region where back electron transfer and deprotonation are competitive, i.e., $k_2[B] = k_{-1}[Fe(II)]$ in Scheme II. Under these conditions, we have shown in an earlier study[24] that the rate law in eq 2 is replaced by the more general form:

$$\ln\frac{[Fe(III)]}{[Fe(III)]_0} - \gamma\left\{1 - \frac{[Fe(III)]}{[Fe(III)]_0}\right\} = k_e't \qquad (15)$$

where γ is the constant parameter which describes how close the system is to the limits of electron-transfer reversibility.[29] The solution of eq 15 by multiple linear regression analysis yields values of the electron-transfer rate constant k_1 (see Experimental Section).

We indeed found that at higher concentrations of 2,6-lutidine, the rate of PMT oxidation did follow the kinetics behavior described by eq 15, as described in the Experimental Section. The second-order rate constant for electron transfer from p-methoxytoluene to $Fe(phen)_3^{3+}$ was evaluated as $k_1 = 6.0$ M^{-1} s^{-1} in acetonitrile.[30] This value compares with $k_1 = 22$ M^{-1} s^{-1} for hexamethylbenzene under essentially the same conditions.[14] To allow direct comparison, the kinetic parameters for electron transfer from these arenes are retabulated in Table IV together with those of other polymethylated benzenes. The free energy of activation $\Delta G^\ddagger$ for electron transfer is evaluated from the rate constant k_1 by:

$$\Delta G^\ddagger = -RT \ln (k_1/Z) \qquad (16)$$

where the collision frequency is taken as 10^{11}.

The quantitative comparison of electron transfer among all of these arenes is most conveniently carried out in the context of Marcus theory expressed as the free energy relationship:[31]

$$\Delta G^\ddagger = \Delta G_0^\ddagger\left\{1 + \frac{\Delta G}{4\Delta G_0^\ddagger}\right\}^2 \qquad (17)$$

where the driving force $\Delta G = \mathcal{F}[E^\circ_{Ar} - E^\circ_{Fe}] + w_p$, and the work term w_r of the reactants is taken to be nil owing to the uncharged arene.[32] The plot in Figure 5 shows the variation of the rate ($\Delta G^\ddagger$) with the change in the driving force ΔG according to the Marcus equation. [Note this free energy plot is normalized to the intrinsic barrier $\Delta G_0^\ddagger$, which is listed in column 5 of Table IV.] The precise fit of the point for p-methoxytoluene in Figure 5 with those of the series of sterically encumbered polymethylated benzenes such as hexamethylbenzene indicates that only electronic effects are important in these electron transfers, which is consistent with an outer sphere activated complex for arene oxidation with $Fe(phen)_3^{3+}$. The dashed line is drawn according to the expectations of the Marcus theory.

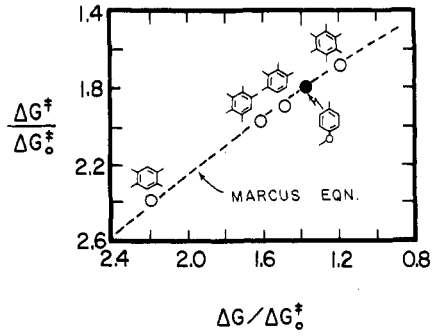

Figure 5. Free energy correlation of the electron-transfer rates ($\Delta G^\ddagger$) from p-methoxytoluene (●) in comparison with those of polymethylbenzenes (○), after normalization to the intrinsic barrier $\Delta G_0^\ddagger$. The dashed line is drawn according to the Marcus equation.

Conclusion

The oxidation of p-methoxytoluene (PMT) by $Fe(phen)_3^{3+}$ in acetonitrile containing pyridine bases B affords aromatic products derived from side chain (methyl) and nuclear (ring) substitution. The products (I and II identified by independent synthesis) together with the stoichiometry accord with the mechanism in Scheme II involving electron transfer (eq 3) followed by the reaction of the p-methoxytoluene cation radical [$PMT^{+}\cdot$] with pyridine (eq 4). The formation of [$PMT^{+}\cdot$] as a transient intermediate is indeed established by the observation of its ESR spectrum when PMT is mixed with $Fe(phen)_3^{3+}$ in the cavity of the spectrometer.

Kinetic studies based on the rate law derived for Scheme II afford the second order rate constant k_1 in eq 3 and the rate constant k_2 in eq 4. The variation of k_2 with changes in the base B from pyridine to 2,6-lutidine, as well as the kinetic isotope effects resulting from deuterium substitution of the methyl substituent, both lead to the conclusion that the products I and II evolve via entirely separate pathways from [$PMT^{+}\cdot$].

Thus side chain substitution derives from the rate-limiting deprotonation of [$PMT^{+}\cdot$] by B in eq 12 to generate the benzylic radical, the subsequent oxidation of which is known to be fast,[33] i.e.,

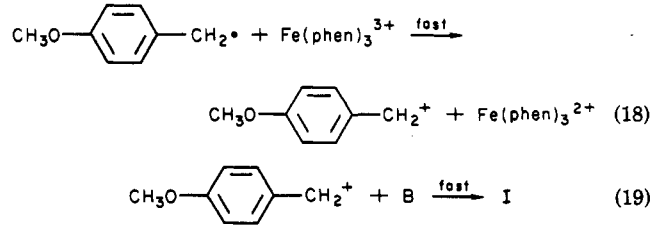

(29) The exact relationship is $\gamma = p/(1 + p)$ where $p = k_{-1}[Fe(III)]_0/k_2[B]$. Note p represents the rate of back electron transfer relative to the rate of deprotonation. For a discussion, see ref 24.

(30) On the same basis, the rate constant for back electron transfer is $k_{-1} = 2.3 \times 10^7$ M^{-1} s^{-1}.

(31) Marcus, R. A. *J. Chem. Phys.* **1956**, *24*, 4966; *Ibid.* **1965**, *43*, 279.

(32) See ref 14 and Klingler, R. J.; Fukuzumi, S.; Kochi, J. K. *ACS Symp. Ser. No. 211*, 117 ff.

(33) Rollick, K. L.; Kochi, J. K. *J. Am. Chem. Soc.* **1982**, *104*, 1319.

The Brønsted analysis (eq 14) shows that the structural changes in B affect the deprotonation rates in eq 12 in measure with the electronic effects shown by their base strength—thus 2,6-lutidine is approximately two times *more* effective than pyridine.

On the other hand, nuclear substitution arises from the rate-limiting nucleophilic addition of B to [$PMT^{+}\cdot$] in eq 13. The formation of the σ-adduct is highly subject to the steric effects of B—thus the hindered 2,6-lutidine is at least ten times *less* effective than pyridine. The subsequent steps leading to II by the loss of proton and oxidation are rapid.[34]

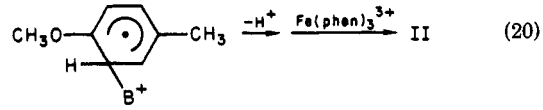

(20)

The results of the kinetic isotope studies do preclude an alternative mechanism for nucleophilic addition via the benzyl cation formed in eq 18, i.e.,

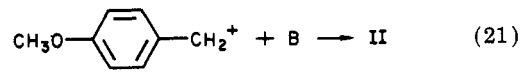

(21)

This type of quantitative analysis of the complex kinetics provides a plausible explanation for an otherwise unusual and pronounced dependence of the oxidative products on the structure of B—namely, the observation of the *N*-benzylpyridinium ion I as the exclusive product from PMT oxidation in the presence of 2,6-lutidine, and the *N*-arylpyridinium ion II from that with pyridine as the base.[35]

The separate evaluation of the electron-transfer rate constant from *p*-methoxytoluene to $Fe(phen)_3^{3+}$ permits the comparison of k_1 with the corresponding rate constants for a variety of polymethylbenzenes. The correlations of the rate data with the linear free energy relationship developed by Marcus theory indicate that both classes of arenes involve an outer sphere activated complex for electron transfer to form the relevant cation–radical intermediate in aromatic oxidations.

Experimental Section

Materials. 1,10-Phenanthroline (Alfa) was recrystallized from toluene prior to use. The tris(phenanthroline)iron(II) complex was prepared from aqueous ferrous sulfate by the addition of 3 equiv of phenanthroline and precipitated with ammonium hexafluorophosphate (Ozark-Mahoning).[8] After the collection of $Fe(phen)_3(PF_6)_2$ as dark red crystals, it was dried over P_2O_5 in vacuo. The blue tris(phenanthroline)iron(III) complex $Fe(phen)_3(PF_6)_3$ was prepared by the oxidation of the ferrous complex with ceric ammonium nitrate (G. F. Smith) in aqueous H_2SO_4 followed by precipitation with NH_4PF_6.

p-Methoxytoluene (Aldrich) was redistilled in vacuo prior to use. The deuteriated derivative *p*-methoxytoluene-α,α,α-d_3 was prepared by the procedure described by Dewar and co-workers.[5] Analysis of the ^1H NMR spectrum indicated a singlet resonance at δ 3.6 for the methoxy group but none (<2%) at δ 2.2 for the methyl substituent. Pyridine and 2,6-lutidine from Matheson, Coleman and Bell were distilled from KOH pellets before use. Acetonitrile (HPLC grade from Fisher Scientific) was further purified by distillation from CaH_2 through a 15-plate Oldershaw column, followed by stirring overnight with $KMnO_4$ and Na_2CO_3 (5 g of each per liter). The mixture was filtered, distilled under reduced pressure, and finally fractionated from P_2O_5 under an argon atmosphere and stored under argon in a Schlenk flask. Acetonitrile purified in this way did not reduce $Fe(phen)_3(PF_6)_3$ upon exposure for prolonged periods. Lithium perchlorate (G. F. Smith Chemical Co.) was further dried in vacuo.

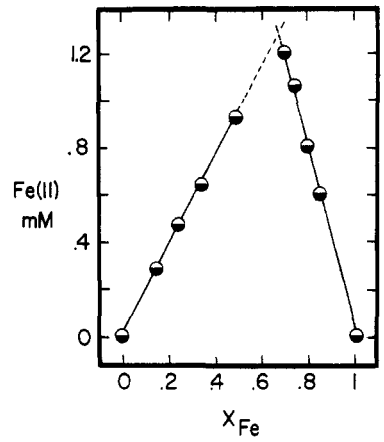

Figure 6. Spectral titration of iron(III) by the method of continuous variations during the oxidation of PMT by $Fe(phen)_3^{3+}$ in acetonitrile.

Synthesis of Side Chain and Nuclear Substitution Products. Authentic samples of the products Ia, Ib, and IIa were synthesized as follows: For Ia and Ib, *p*-methoxybenzyl alcohol was converted to the bromide by Gonzales' method[36] using a slight excess of PBr_3 in hexane. The crude benzylic bromide was added to either neat pyridine or 2,6-lutidine. An oily layer separated upon stirring the mixture at room temperature overnight. After trituration with diethyl ether, the solid was dissolved in hot water, followed by quantitative precipitation with NH_4PF_6. ^1H NMR spectrum (CD_3CN) for Ia: δ 6.99 (d, J = 9 Hz, 1 H), 7.40 (d, J = 9 Hz, 1 H), 7.40 (d, J = 9 Hz, 1 H), 6.99 (d, J = 9 Hz, 1 H), 5.62 (s, 2 h), 3.79 (s, 3 H), 8.70 (d, J = 5 Hz, 1 H), 7.99 (br t, J = 7 Hz, 1 H), 8.48 (t, J = 8 Hz, 1 H), δ 7.99 (br t, J = 7 Hz, 1 H), 8.70 (d, J = 5 Hz, 1 H). For Ib: δ 6.90 (d, J = 6 Hz, 1 H), 6.94 (d, J = 6 Hz, 1 H), 6.94 (d, J = 6 Hz, 1 H), 6.90 (d, J = 6 Hz, 1 H), 5.67 (s, 2 H), 3.76 (s, 3 H), 7.79 (d, J = 8 Hz, 1 H), 8.29 (t, J = 8 Hz, 1 H), 7.79 (d, J = 8 Hz, 1 H), 2.71 (s, 3 H), 2.71 (s, 3 H) relative to internal Me_4Si. The compound Ib upon recrystallization from ethyl acetate afforded colorless crystals, mp 165–167 °C. Anal. Calcd for $C_{15}H_{18}NOPF_6$: C, 48.26; H, 4.87; N, 3.75. Found: C, 48.10; H, 4.69; N, 3.53. [All analyses were performed by Midwest Microlab, Indianapolis.]

For compound IIa, *N*-(2,4-dinitrophenyl)pyridinium chloride was synthesized by the method of Fisher and Hamer.[37] It was converted to the ring-opened $[(2\text{-}CH_3O\text{-}5\text{-}CH_3C_6H_3)NHCH{=}CHCH{=}CHCH{=}NH(C_6H_3\text{-}5\text{-}CH_3\text{-}2\text{-}OCH_3]^+Cl^-$ by treatment with 2 equiv of 5-methyl-2-anisidine according to Marvell.[11] Treatment of this salt with triethylamine to induce cyclization and elimination[11] afforded 2-(5-methylanisyl)pyridinium chloride. Metathesis to the hexafluorophosphate salt was carried out by the same procedure described for Ia above: ^1H NMR spectrum (CD_3CN) of IIa: δ 7.36 (m, 1 H), 7.48 (d, J = 8 Hz, 1 H), 7.22 (d, J = 8 Hz, 1 H), 2.37 (s, 3 H), 3.81 (s, 3 H), 8.76 (d, J = 8 Hz, 1 H), 8.14 (dd, J = 7, 8 Hz, 1 H), 8.65 (t, J = 7 Hz, 1 H), 8.14 (dd, J = 7, 8 Hz, 1 H), 8.76 (d, J = 8 Hz, 1 H) relative to HCD_2CN at 1.930 ppm. The ^{13}C NMR spectrum (CH_3CN) of IIa: δ 151, 133, 135, 132, 128, 114, 20.4, 57.4, 147, 129, 148, 129, 147. Recrystallization of IIa from ethyl acetate afforded colorless crystals, mp 115–118 °C. Anal. Calcd for $C_{13}H_{14}NOPF_6$: C, 45.22; H, 4.09; N, 4.06. Found: C, 45.42; H, 3.93; N, 3.95.

Stoichiometry of PMT Oxidation with Iron(III). The stoichiometry of the oxidation was determined by two independent methods involving the spectral titration of the iron(III) oxidant and the consumption of *p*-methoxytoluene by gas chromatography.

Spectral Titration. The method of continuous variations[10] was used to monitor the stoichiometry of the reaction of $Fe(phen)_3^{3+}$ with PMT. Solutions of 2×10^{-3} M $Fe(phen)_3^{3+}$ and 2×10^{-3} M PMT in acetonitrile were mixed in varying proportions while

(34) This sequence cannot be distinguished at this juncture from the reverse, i.e., oxidation followed by proton loss.

(35) For other studies of selectivity and kinetic isotope effects in arene oxidation by chemical and electrochemical methods, see: Baciocchi, E.; Eberson, L.; Rol, C. *J. Org. Chem.* **1982**, *47*, 5106.

(36) Gonzales, A. G.; Aguiar, J. M.; Martin, J. D.; Rodriguez, M. L. *Tetrahedron Lett.* **1976**, 205.

(37) Fisher, N. I.; Hamer, F. M. *J. Chem. Soc.* **1933**, 189.

keeping the total volume constant at 2 mL. The mole fraction X_{Fe} of $Fe(phen)_3^{3+}$ was varied from 0.15 to 0.85 by using eight samples as shown in Figure 6. In addition, a small amount of pyridine or lutidine was added in amounts equivalent to the iron(III) to be consumed. The absorbance at 560 nm and/or 550 nm was recorded after 24 h, which allowed the iron(II) concentration to be computed from the extinction coefficients at 560 nm of ϵ 1860 and 680 M^{-1} cm^{-1} and at 550 nm of ϵ 3170 and 620 M^{-1} cm^{-1} for $Fe(phen)_3^{2+}$ and $Fe(phen)_3^{3+}$, respectively. A typical plot of iron(II) produced against the mole fraction of initial iron(III) hereafter given as $[Fe(III)]_0$ is illustrated in Figure 6. The maximum X_m at 0.681 corresponded to $X_m = (1 - X_m)S_1$ where the stoichiometry S = [Fe(III)]/[PMT] = 2.1. **Gas Chromatography.** The consumption of PMT was determined directly by analysis on a 20-ft cross-linked methylsilicone capillary column with a Hewlett-Packard 5790A/3390 chromatograph/integrator. The reaction mixtures consisted of 0.1 mm $Fe(phen)_3^{3+}$, 0.05 mmol PMT, and 0.1 mmol pyridine in 2 mL acetonitrile. After ~5–10 days, the solution was treated with a weighed quantity of 1,3,5-tri-*tert*-butylbenzene as an internal standard. After analysis of the mixture by gas chromatography, the solution was treated with diethyl ether to precipitate the iron salts which were then analyzed spectroscopically at 550 and 560 nm after dissolution in acetonitrile. The stoichiometry determined by this method was S = [Fe(II)]/([PMT]$_0$ − [PMT]) = 1.8.

Isolation and Characterization of PMT Oxidation Products. In a typical procedure, a homogeneous solution containing PMT, $Fe(phen)_3^{3+}$, and base in 20 mL acetonitrile and in the amounts listed in Table I was allowed to stand at room temperature for a prolonged period. A 2-mL aliquot of the reaction mixture was set aside for quantitative analysis (vide infra). The remainder was added slowly to ~400 mL of diethyl ether to separate the iron salts, which were removed by filtration. The clear filtrate was concentrated in vacuo to afford an oily solid which was washed several times with hexene and dried in vacuo. The solid was dissolved in acetonitrile-d_3 for NMR analysis (vide infra). The iron precipitate was redissolved in acetonitrile and analyzed spectrophotometrically at 550 and 560 nm (vide supra). One half of the 2-mL aliquot was treated with a weighed quantity of 1,3,5-tri-*tert*-butylbenzene as an internal standard for gas chromatographic analysis of PMT (vide supra). The same solution was then treated with a weighed quantity of triphenylmethane for quantitative ^1H NMR analysis by the following procedure. The solvent was removed by evaporation under a stream of argon, and acetonitrile-d_3 was added to the residue for examination on a Nicolet NT-360 spectrometer. For the product with pyridine as the base, the ^1H NMR spectrum showed singlet resonances at δ 5.62 (corresponding to Ia) and 3.82 (corresponding to IIa) which were integrated relative to the internal standard at δ 5.54. Since IIa was the major isomer its ^1H NMR spectrum was examined relative to that of the authentic sample (vide supra), and the chemical shifts are presented for comparison in the same order as: δ 7.37 (s, 1 H), 7.47 (d, J = 8 Hz, 1 H), 7.23 (d, J = 8 Hz, 1 H), 2.37 (s, 3 H), 3.82 (s, 3 H), 8.77 (m, 1 H), 8.15 (m, 1 H), 8.66 (m, 1 H), 8.15 (m, 1 H), 8.77 (m, 1 H). Similarly, the ^{13}C NMR spectrum: δ 151, 133, 135, 132, 128, 114, 20.3, 57.4, 147, 129, 148, 129, 147. For the product with 2,6-lutidine as the base, only a singlet resonance was observed at δ 5.66 (corresponding to Ib). The ^1H NMR spectrum is presented in the same order as that of authentic Ib (vide supra): δ 6.91 (d, J = 7 Hz, 1 H), 6.93 (d, J = 7 Hz, 1 H), 6.93 (d, J = 7 Hz, 1 H), 6.91 (d, J = 7 Hz, 1 H), 5.66 (s, 2 H), 3.76 (s, 3 H), 7.78 (d, J = 8 Hz, 1 H), 8.28 (t, J = 8 Hz, 1 H), 7.78 (d, J = 8 Hz, 1 H), 2.71 (s, 3 H), 2.71 (s, 3 H). As an additional check on these analyses, the other half of the 2-mL aliquot was treated as described above to ensure the absence of spurious resonances introduced by the internal standards.

Kinetic Measurements. Solutions of ~0.1 mM $Fe(phen)_3^{3+}$ in acetonitrile were examined spectrophotometrically under pseudo-first-order conditions with >10-fold excess PMT (8–60 mM) and varying amounts of base (pyridine or 2,6-lutidine at 4–125 mM) in a 1.0-cm quartz cuvette, preflushed with argon. [The same results were obtained when Schlenk techniques were used to exclude air.] The absorbance of either $Fe(phen)_3^{2+}$ at 510 nm (ϵ 1.1 × 10^4 M^{-1} cm^{-1}) or $Fe(phen)_3^{3+}$ at 650 nm (ϵ 540 M^{-1} cm^{-1}) was monitored at intervals ranging from 1 to 10 s allowed by the use of a Hewlett-Packard 8450A UV–vis spectrometer equipped with a diode array detector for rapid scan. The kinetics were generally followed to beyond 99% conversions. The absorbance A was related to the extent of reaction given as: x = [Fe(III)]/[Fe(III)]$_0$ = $(A_\alpha - A_t)/(A_\alpha - A_0)$. The rate constants k_e for those reactions carried out under pseudo-first-order conditions were obtained from a plot of $-\ln x + G(x - 1)$ against time t (see derivation of kinetics and data treatment below). Control runs in the absence of either PMT or added base were used to justify the necessity of both components in the observed kinetics. In each case, the consumption of [Fe(III)] was negligible in the controls when compared to the rate of iron(III) consumption in the presence of both PMT and base.

Derivation of the Rate Expressions for the Kinetics of Electron-Transfer Oxidation. The rate expression given in eq 1 derives from the mechanism in Scheme I (when PMT and the base are in >10-fold excess relative to $Fe(phen)_3^{3+}$) in the following manner. The disappearance of iron(III) is given by:

$$d[Fe(III)]/dt = -2k_2[PMT^{+}\cdot][B] \quad (22)$$

when electron transfer in eq 3 is in full equilibrium and the stoichiometric consumption of $Fe(phen)_3^{3+}$ for each mole of PMT is 2. Using the steady-state assumption for $[PMT^{+}\cdot]$ yields:

$$[PMT^{+}\cdot] = (k_1/k_{-1})[Fe(III)][PMT]/[Fe(II)] \quad (23)$$

and eq 22 becomes:

$$d[Fe(III)][Fe(II)]/[Fe(III)] = -(2k_2k_1/k_{-1})[PMT][B] \quad (24)$$

Substitution of [Fe(II)] = C^0 − [Fe(III)], where C^0 = ([Fe(II)]$_0$ + [Fe(III)]$_0$), and integration from t_{exp} = 0–t, or ([Fe(III)]$_0$–[Fe(III)]) yields:

$$C^0 \ln \{[Fe(III)]/[Fe(III)]_0\} + [Fe(III)] - [Fe(III)]_0 = -(2k_1k_2/k_{-1})[PMT][B]t \quad (25)$$

where t_{exp} is the time from which the absorbance measurements actually commenced. [Note for rapid reactions it is experimentally not feasible to set precisely $t_{exp} = t = 0$.] If x = [Fe(III)]/[Fe(III)]$_0$, eq 25 simplifies to:

$$-C^0 \ln x + [Fe(III)]_0(x - 1) = (2\ k_1k_2/k_{-1})[PMT][B]t \quad (26)$$

The initial concentration of iron(III) can be expressed in terms of the absorbance A as:

$$[Fe(III)]_0 = C^0(1 - A_0/A_\infty)/(1 - \epsilon_{III}/\epsilon_{II}) \quad (27)$$

since $C^0 = A_\alpha/\epsilon_{II}$ = ([Fe(III)]$_0$ + [Fe(II)]$_0$) and A_0 = (ϵ_{II}[Fe(II)]$_0$ + ϵ_{III}[Fe(III)]$_0$), where ϵ_{II} and ϵ_{III} refer to the extinction coefficients of $Fe(phen)_3^{2+}$ and $Fe(phen)_3^{3+}$, respectively, at the monitoring wavelength. Substitution of eq 27 into eq 26 affords:

$$-\ln x + (x - 1)(1 - A_0/A_\infty)/(1 - \epsilon_{II}/\epsilon_{III}) = (2\ k_1k_2/k_{-1})([PMT][B]/C_0)t \quad (28)$$

If we set $(1 - A_0/A_\alpha)/(1 - \epsilon_{II}/\epsilon_{III}) = G$, then eq 28 is simply:

$$-\ln x + G(x - 1) = (2\ k_1k_2/k_{-1})([PMT][B]/C^0)t = k_e t \quad (29)$$

It is important to note that the factor G allows for any uncertainty in the time of mixing (i.e., $t_{exp} \neq t = 0$) to be taken into account explicitly, especially for rapid reactions of the type examined in this study.[38]

Treatment of the Kinetic Data. The data collected on the UV–vis spectrometer was transferred to a Digital Equipment Corporation 11/23 computer. The interface allowed the absorbance data to be converted to x (vide supra), and later to the functions in x and $(1 - x)$ which were treated as independent variables by using a multiple linear regression program in which x was the dependent variable in eq 29. The regression analysis was performed for each experiment at 3 values of x ranging from 1.0 to 0.5, 1.0 to 0.2, and 1.0 to 0.1, i.e., conversions of 50%, 75% and 90%, respectively. This procedure ensured that uniform kinetics were obtained throughout each run. The validity of the procedure was indicated by the constancy of k_e up to high conversions. Furthermore the same reliability of the method was shown by the invariance of k_e evaluated in kinetic runs at different

(38) Equation 22 should be compared with the general rate expressions derived earlier,[24] when $p = k_{-1}C^0/k_2[B]$ approaches infinity, i.e., G = 1.

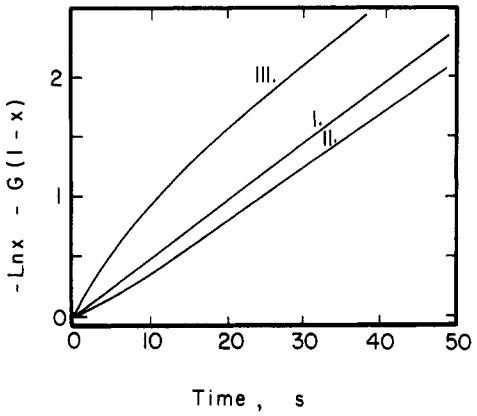

Figure 7. Kinetic treatment according to eq 22 of the rate data for the oxidation of 1.8×10^{-2} M *p*-methoxytoluene, 1.25×10^{-1} M pyridine, and 1.3×10^{-4} M $Fe(phen)_3^{3+}$ in acetonitrile containing 0.1 M $LiClO_4$. Curve I represents $G = (1 - A_0/A_\infty)/(1 - \epsilon_{III}/\epsilon_{II}) = 0.72$. Curve II represents $G = 1.0$. Curve III represents $G = 0$.

Table V. Electron Transfer Kinetics for PMT[a]

lutidine, mM	$Fe(phen)_3^{3+}$, mM	G	γ	P	k_1 M^{-1} s^{-1}
21.6	0.124	0.83	0.76	10.8	6.7
43.2	0.131	0.78	0.66	5.7	6.9
43.2	0.134	0.80	0.69	7.4	7.7
21.6	0.134	0.85	0.76	9.5	5.6

[a] In acetonitrile solutions containing 18.5 mM PMT and 0.1 M $LiClO_4$ at 25 °C.

concentrations of either PMT or pyridine. In practice we generally found eq 29 to be the experimentally feasible form of the rate expression in eq 2 (in which $G = 1$), since most of the oxidations were too fast to set accurately t_{exp} to the zero point of mixing at $t = 0$. The practical effect of the correction using G is illustrated by the true line I in Figure 7 with the slope k_e. By comparison, curve II represents the same rate data plotted as eq 2 (i.e., $G = 1$) and shows an initial concave behavior owing to the error in determining $t = 0$. For comparison, curve III is the rate data plotted as $-\ln x$ vs. time (i.e., $G = 0$).

Evaluation of the Electron-Transfer Rate Constant for PMT. The kinetics runs for the determination of the deprotonation rate constant k_H in eq 7 were typically carried out at base concentrations which were sufficiently *low* so that the rate expression in eq 2 (or equivalently eq 29) applied. In terms of the mechanism in Scheme II, this condition represented electron transfer in full *equilibrium* followed by rate-limiting proton transfer, i.e., $k_2[B] << k_{-1}[Fe(II)]$. As such, it could be readily attained with those methylarenes such as PMT in which back electron transfer (k_{-1}) is faster than deprotonation (k_2) of the methylarene$^{+\cdot}$. At the same time however, it made difficult the determination of k_1 by the use of sufficiently *high* base concentrations to attain a kinetics condition in which electron transfer was rate limiting, i.e., $k_2[B] >> k_{-1}[Fe(II)]$. Consequently we were forced to treat the intermediate kinetics situation in which the general rate expression in eq 15 applied, viz., base concentrations sufficient to allow $k_2[B] \simeq k_{-1}[Fe(II)]$, as listed in Table V. In eq 15, the experimental rate constant $k_e' = 2k_{-1}[PMT]_0/(1 + p)$, where $p = k_{-1}[Fe(III)]_0/k_2[B]$. The coefficient γ in eq 15 was obtained from the linear regression, and it equals $Gp/(1 + p)$. Reliable values of k_1 were obtained in this manner as listed in column 6. The full details of the kinetics treatment for the rate expression in eq 15 are described elsewhere.[24]

Electrochemical Measurements of PMT and $Fe(phen)_3^{3+}$. The standard oxidation potentials of PMT and $Fe(phen)_3^{2+}$ were measured by cyclic voltammetric methods in which E° was taken as $(E_p^a + E_p^c)/2$ where E_p^a and E_p^a and E_p^c are the peak potentials of the anodic and cathodic waves, respectively.[39] Unfortunately the cyclic voltammogram of *p*-methoxytoluene is irreversible in acetonitrile owing to the rapid reaction of [PMT$^{+\cdot}$] with this solvent. However a reversible cyclic voltammogram could be obtained at relatively high scan rates in trifluoroacetic acid containing 5 %vol trifluoroacetic anhydride. Using a gold microelectrode by a technique described earlier,[40] a peak separation of 80–90 mV could be obtained from which $E^\circ_{Ar} = 1.25_6 \pm 0.029$ for PMT. For comparison, the values of E°_{Ar} for 2-methoxytoluene, 3-methoxytoluene, and 2,6-dimethoxytoluene are 1.32 ● 0.02, 1.44 ± 0.01, and 1.30 ± 0.01 V vs. $Ag/AgClO_4$ in trifluoroacetic acid containing 5 %vol trifluoroacetic anhydride. Under the same conditions E°_{Fe} for $Fe(phen)_3^{3+}$ is 0.870 ± 0.002 V vs. $Ag/AgClO_4$. The corresponding values for the tris 5-chloro- and 5-nitrophenanthroline derivatives are 0.963 ± 0.001 and 1.073 ± 0.002 V.

Evaluation of the Free Energy Terms. For the application to the Marcus equation, the free energy change ΔG was determined from the standard oxidation potentials, E°_{Ar} and E°_{Fe}, using the expression $\Delta G = \mathcal{F}[E^\circ_{Ar} - E^\circ_{Fe}] + w_p$. The work term of the product w_p was taken to be 1.7 kcal mol^{-1}, as previously described.[14] Unfortunately there is ambiguity as to the proper values of E°_{Ar} and E°_{Fe} to use, since the standard oxidation potential of methylbenzenes cannot be measured by cyclic voltammetry in acetonitrile. Two approaches have been employed. In the previous study,[14] we uniformly applied a solvent correction of 0.12 V to the values of E°_{Ar} measured in trifluoroacetic acid. Alternatively, E°_{Fe} (0.87 V vs. $Ag/AgClO_4$) as measured in trifluoroacetic acid can be used directly with E°_{Ar} in the same solvent (listed in Table IV) on the (tenuous) basis that the solvent effect in the two redox couples would cancel out. The values of the intrinsic barrier ΔG_0^* calculated from eq 17 using this assumption are listed in column 5 of Table IV. Note that these values for hexamethylbenzene, pentamethylbenzene, durene, and prehnitene differ somewhat from those presented earlier[14] owing to the ambiguity in the solvent correction mentioned above; but otherwise the conclusions are the same.

Electron Spin Resonance Study of [PMT$^{+\cdot}$] as an Intermediate. Since arene cation radicals are known to be much more persistent in trifluoroacetic acid than in acetonitrile,[41] the observation of [PMT$^{+\cdot}$] during the thermal reaction of PMT and $Fe(phen)_3^{3+}$ was carried out in the following manner. A trifluoroacetic acid solution of 1.3×10^{-3} M PMT contained in an ESR tube was degassed and then frozen. A solution of 2.3×10^{-3} M $Fe(phen)_3(PF_6)_3$ made up in trifluoroacetic acid containing approximately 5 %vol water was added to the tube, quickly degassed and frozen. The sealed tube was warmed rapidly just until it thawed. The contents were rapidly mixed and the ESR spectrum in Figure 4a was recorded at a fast scan rate since the oxidation under these conditions was complete within a few minutes. The relatively broad lines in the spectrum could thus be attributed to the less than optimum conditions for these spectral measurements. The isotropic value of 2.0033 is based on an external DPPH standard. The computer simulated spectrum in Figure 4b is based on the proton hyperfine splittings listed in ref 12, and a peak-to-peak line width of 1.7 gauss. A broad underlying ESR signal with 25% of the amplitude was imposed as a background for the simulation.

Acknowledgment. We thank W. Lau and K. Srinivasan for help with the ESR experiments, C. Amatore for the electrochemical measurements and many helpful discussions, J. Goncalves for the computer interface of the spectral data, and the National Science Foundation for financial support.

Registry No. Ia·PF_6, 91084-08-1; Ib·PF_6, 91084-10-5; IIa·PF_6, 91084-12-7; *p*-methoxytoluene, 104-93-8; tris(phenanthroline)-iron(III), 13479-49-7; pyridine, 110-86-1; 2,6-lutidine, 108-48-5; deuterium, 7782-39-0.

Supplementary Material Available: Table of [Fe(III)] as a function of time for Figure 2a (1 page). Ordering information is given on any current masthead page.

(39) Klingler, R. J.; Kochi, J. K. *J. Phys. Chem.* **1981**, *85*, 1731.

(40) Howell, J. O.; Goncalves, J.; Amatore, C.; Klasinc, L.; Wightman, R. M.; Kochi, J. K. *J. Am. Chem. Soc.*, in press.

(41) Compare Hammerich, O.; Moe, N. S.; Parker, V. D. *J. Chem. Soc., Chem. Commun.* **1972**, 156.